Available online at www.sciencedirect.com
ScienceDirect
Inorganica Chimica Acta 361 (2008) 400–406
Inorganica Chimica Acta
www.elsevier.com/locate/ica

Note

Syntheses, crystal structures, and magnetic properties of two novel $Ni(mnt)_2$-based molecular magnetic materials containing substituted triphenylphosphinium

Jiarong Zhou [a], Chunlin Ni [a,b,*], Linliang Yu [a,b], Lemin Yang [a,b]

[a] Department of Applied Chemistry, College of Science, South China Agricultural University, 510642 Guangzhou, PR China
[b] Centre of Inorganic Functional Materials, South China Agricultural University, 510642 Guangzhou, PR China

Received 20 February 2007; received in revised form 19 May 2007; accepted 8 July 2007
Available online 13 July 2007

Abstract

Two novel molecular magnetic materials, $[RBzTPP][Ni(mnt)_2]$ (mnt^{2-} = maleonitriledithiolate, $[RBzTPP]^+$ = 4-R-benzyltriphenylphosphinium; R = CN (**1**), Cl (**2**)) were synthesized and characterized by X-ray diffraction, IR spectroscopy, and magnetic susceptibility measurements. In crystal of **1**, the $[Ni(mnt)_2]^-$ anions form a dimer *via* Ni···S and π···π stacking interactions between $Ni(mnt)_2$ planes, and the C–H···Ni and C–H···N H-bonding interactions are found between the $[Ni(mnt)_2]^-$ anions and the neighboring $[CNBzTPP]^+$ cations. The anions and cations of **2** stack into well-segregated columns in the solid state; and the Ni(III) ions form a 1D alternating chain in a $Ni(mnt)_2$ column through intermolecular Ni···S, or π···π interactions with the Ni···Ni distances of 3.900, 4.198, and 4.165 Å. Magnetic susceptibility measurements for these complexes in the temperature range 1.8–300 K show that the overall magnetic behavior for **1** and **2** indicates the presence of antiferromagnetic interaction, but **1** exhibits an activated magnetic behavior in the high-temperature (HT) region together with a Curie tail in the low-temperature (LT) region.

Keywords: Bis(maleonitriledithiolato)nickelate complex; Substituted triphenylphosphinium; Crystal structure; H-Bonding interaction; Magnetic properties

1. Introduction

Great interest in recent years has been directed toward the development of structural and functional analogues of molecular solids based on metal dithiolene complexes by virtue of their ability to assemble in the solid state with short sulfur–sulfur, metal–sulfur or π···π stacking interactions [1–5]. The planar anion $[M(mnt)_2]^-$ (M = Ni, Pd or Pt) had been proved to be good building block to construct molecular materials, which exhibit versatile magnetic properties such as ferromagnetic ordering, magnetic transition from ferromagnetic to diamagnetic coupling, meta-magnetism, and spin-Peierls-like transitions [6–11]. Of key importance in design of such materials is to find more suitable multifunctional organic cations to tune the crystal stacking structure of the $[Ni(mnt)_2]^-$ anion. One of the advantages of using organic cation as countercation for $[M(mnt)_2]^-$ monoanion is that the topology and size of the countercation in $Ni(mnt)_2$ complex may play an important role in controlling the stacking pattern of anions and cations, which further influence the magnetic properties. Some surprising results in our previous systematic studies on a series of ionic complexes composed of $[Ni(mnt)_2]^-$ anion and substituted benzylpyridinium cation prompted us to investigate the effects of some larger organic cations on the stacking pattern of $Ni(mnt)_2$ complexes [12–20]. We herein introduced two substituted benzyltripenylphosphiniums

* Corresponding author. Address: Department of Applied Chemistry, College of Science, South China Agricultural University, 510642 Guangzhou, PR China. Tel.: +86 20 85282568; fax: +86 20 85282366.
E-mail address: niclchem@scau.edu.cn (C. Ni).

0020-1693/$ - see front matter © 2007 Elsevier B.V. All rights reserved.
doi:10.1016/j.ica.2007.07.004

Table 1
Crystal data and structure refinement for **1** and **2**

Compound	**1**	**2**
Empirical formula	$C_{34}H_{21}N_5NiPS_4$	$C_{33}H_{21}N_4NiClPS_4$
Formula weight	717.48	726.91
T (K)	293(2)	293(2)
Wavelength (Å)	0.71073	0.71073
Crystal system	triclinic	monoclinic
Space group	$P\bar{1}$	$P2_1/c$
a (Å)	11.815(2)	15.767(3)
b (Å)	12.613(2)	23.393(4)
c (Å)	12.120(2)	21.682(3)
α (°)	114.68(1)	90
β (°)	101.49(1)	123.91(1)
γ (°)	90.77(1)	90
Volume (Å^3)	1677.9(4)	6637.2(19)
Z	2	8
D_{calc} (mg/m^3)	1.420	1.455
Absorption coefficient (mm^{-1})	0.907	0.995
F(000)	734	2968
Crystal size (mm)	$0.40 \times 0.30 \times 0.30$	$0.48 \times 0.34 \times 0.17$
Reflections collected	8354	39411
Independent reflections (R_{int})	5787 (0.029)	13485 (0.032)
Refinement method	full-matrix least-squares on F^2	full-matrix least-squares on F^2
Data/restraints/parameters	5787/0/307	13485/0/793
Goodness of fit on F^2	1.040	1.001
Final R indices [$I > 2\sigma(I)$]	$R_1 = 0.0547$, $wR_2 = 0.1179$	$R_1 = 0.0375$, $wR_2 = 0.0789$
Final R indices (all data)	$R_1 = 0.0826$, $wR_2 = 0.1289$	$R_1 = 0.0675$, $wR_2 = 0.0914$

into the Ni(mnt)$_2$ system and obtained two newly prepared Ni(mnt)$_2$-based molecular magnetic materials: [CNBzTPP][Ni(mnt)$_2$] (**1**) and [ClBzTPP][Ni(mnt)$_2$] (**2**), whose syntheses, crystal structures and magnetic properties are described. Although these molecular solids show antiferromagnetic coupling behavior, **1** exhibits an activated magnetic behavior in the high-temperature (HT) region together with a Curie tail in the low-temperature (LT) region.

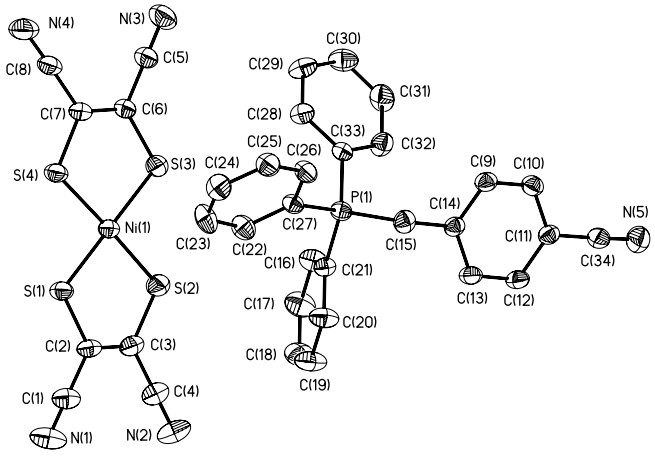

Fig. 1. ORTEP plot (30% probability ellipsoids) showing the molecular structure of **1**.

2. Experimental

All reagents and chemicals were purchased from commercial sources and were used without further purification. Disodium maleonitriledithiolate (Na$_2$mnt) was synthesized by a published procedure [21]. 4-Cyanobenzyltriphenylphosphinium bromide ([CNBzTPP]Br) and 1-(4′-chlorobenzyl) triphenylphosphinium bromide ([ClBzTPP]Br) were prepared by the literature methods [22]. A similar method for preparing [BzTPP]$_2$[Ni(mnt)$_2$] was used to prepare [CNBzTPP]$_2$[Ni(mnt)$_2$] and [ClBzTPP]$_2$[Ni(mnt)$_2$] [23].

2.1. Synthesis of [CNBzTPP][Ni(mnt)$_2$] (1)

An acetone solution (10 cm^3) of I$_2$ (240 mg, 0.93 mmol) was slowly added to an acetone solution (20 cm^3) of [CNBzTPP]$_2$[Ni(mnt)$_2$] (1645 mg, 1.50 mmol) and the mixture was stirred for 12 h. MeOH (120 cm^3) was then added, and the mixture allowed to stand overnight, 915 mg of black micro-crystals formed were filtered off, washed with MeOH and dried in vacuum. Yield: 85%. *Anal*. Calc. for $C_{34}H_{21}N_5NiPS_4$: C, 56.92; H, 2.95; N, 9.76. Found: C, 56.87; H, 3.06; N, 9.59%. IR spectrum (cm^{-1}): ν(CN), 2226, 2208 s; ν(C=C) of mnt^{2-}, 1437 s.

2.2. Synthesis of [ClBzTPP][Ni(mnt)$_2$] (2)

The procedure for preparing **2** is similar to that for **1**. Yield: 87%. *Anal*. Calc. for $C_{33}H_{21}N_4NiClPS_4$ (**2**): C, 54.53; H, 2.91; N, 7.71. Found: C, 54.47; H, 2.98; N, 7.54%. IR (KBr, cm^{-1}): IR spectrum (cm^{-1}): ν(CN), 2206 s; ν(C=C) of mnt^{2-}, 1436 s.

Table 2
Selected bond lengths (Å) and bond angles (°) for **1**

Bond length (Å)			
Ni(1)–S(1)	2.142(1)	S(1)–C(2)	1.712(4)
Ni(1)–S(2)	2.140(1)	S(2)–C(3)	1.711(5)
Ni(1)–S(3)	2.143(1)	S(3)–C(6)	1.714(4)
Ni(1)–S(4)	2.133(1)	S(4)–C(7)	1.728(5)
N(1)–C(1)	1.130(8)	P(1)–C(15)	1.813(4)
N(2)–C(4)	1.134(7)	P(1)–C(21)	1.784(4)
N(3)–C(5)	1.135(7)	P(1)–C(27)	1.790(4)
N(4)–C(8)	1.138(7)	P(1)–C(33)	1.795(4)
Bond angles (°)			
S(1)–Ni(1)–S(2)	92.48(5)	P(1)–C(15)–C(14)	117.9(3)
S(1)–Ni(1)–S(4)	87.11(4)	P(1)–C(21)–C(16)	121.4(3)
S(2)–Ni(1)–S(3)	88.28(4)	P(1)–C(21)–C(20)	119.1(3)
S(3)–Ni(1)–S(4)	92.23(5)	P(1)–C(27)–C(26)	118.8(3)
Ni(1)–S(1)–C(2)	103.28(18)	P(1)–C(27)–C(22)	121.6(3)
Ni(1)–S(2)–C(3)	103.07(16)	P(1)–C(33)–C(28)	119.7(3)
Ni(1)–S(3)–C(6)	103.49(18)	P(1)–C(33)–C(32)	120.6(3)
Ni(1)–S(4)–C(7)	103.30(16)	C(15)–P(1)–C(21)	110.76(17)

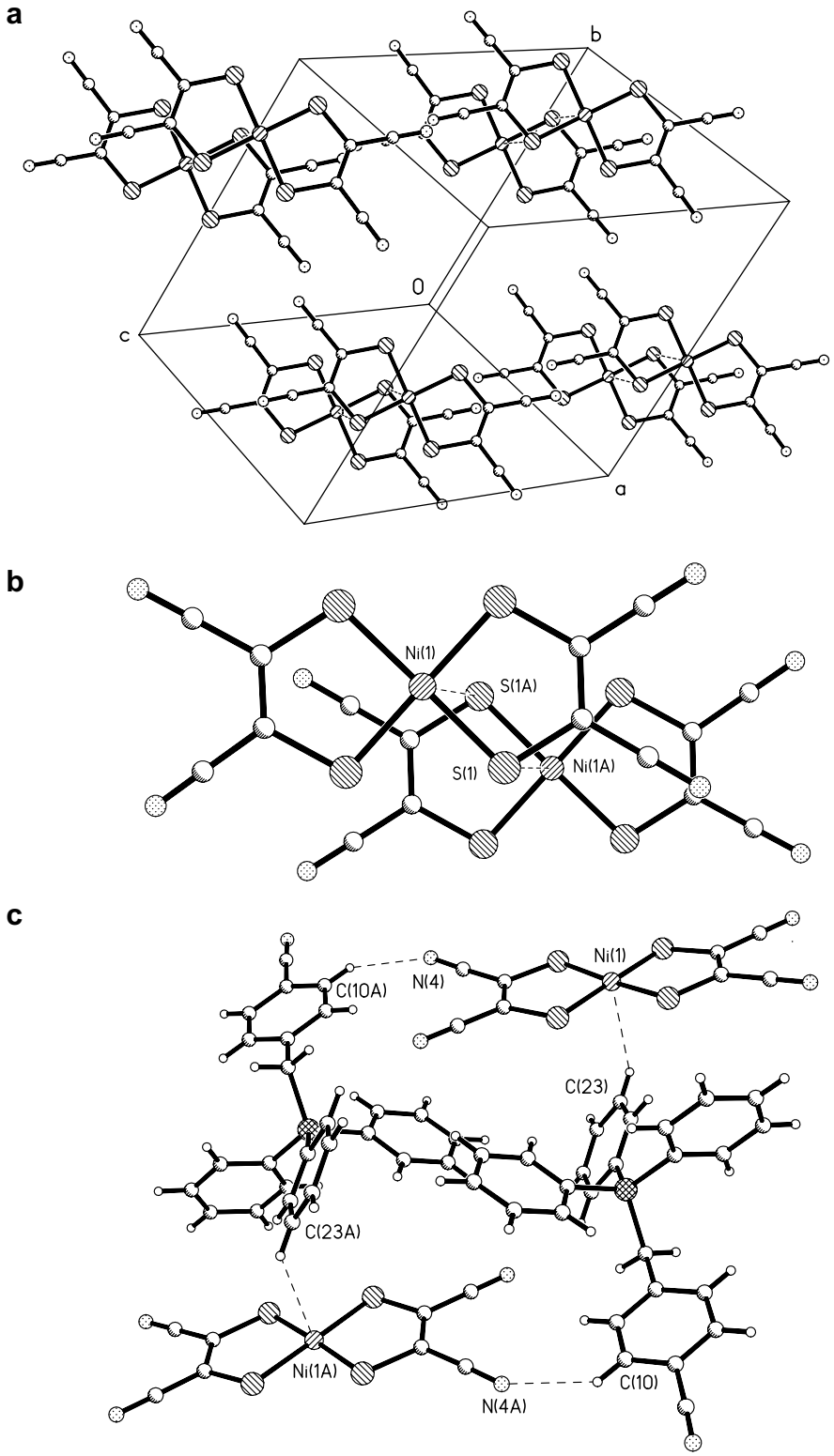

Fig. 2. (a) The packing diagram of the anions for **1**. (b) Mode of overlapping of $[Ni(mnt)_2]^-$ anions for **1**. (c) The weak C–H···Ni and C–H···N H-bonding interactions (dashed lines) between the anions and cations for **1**.

The black single crystals suitable for the X-ray structure analysis were obtained by slowly evaporating the MeCN and *i*-PrOH (v/v = 2:1) mixed solution of **1** and **2** about 15 days at room temperature.

2.3. Instrumental procedures

IR spectra were recorded on a Nicolet FT-IR spectrophotometer in 4000–400 cm^{-1} regions as KBr pellets.

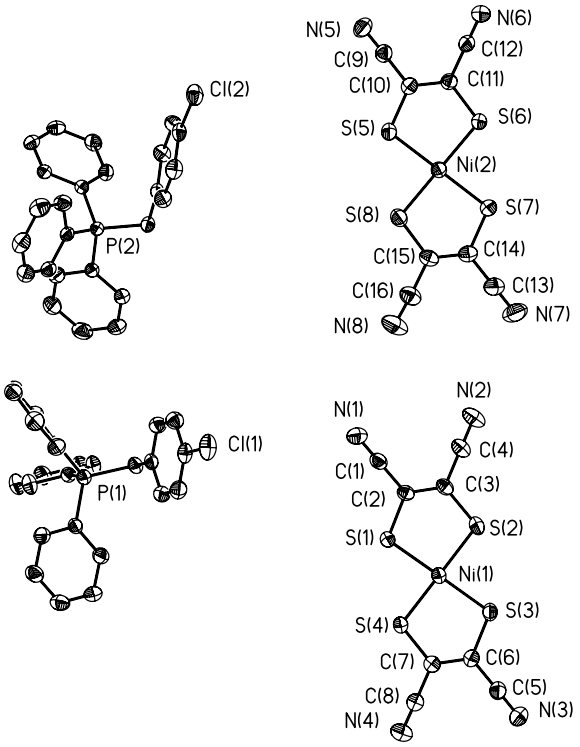

Fig. 3. ORTEP plot (30% probability ellipsoids) showing the molecular structure for **2**.

Elemental analyses of C, H, and N were run on a Model 240 Perkin–Elmer C H N instrument. Magnetic susceptibility data on polycrystals sample were collected over the temperature range of 1.8–300 K using a Quantum Design MPMS-7S super-conducting quantum interference device (SQUID) magnetometer, and diamagnetic corrections were made using Pascal's constants.

2.4. Crystal structure determination

Single crystals of [CNBzTPP][Ni(mnt)$_2$] (**1**) and [ClBzTPP][Ni(mnt)$_2$] (**2**) were mounted on a Bruker Smart APEX CCD area detector using graphite-monochromated Mo Kα radiation ($\lambda = 0.71073$ Å) by ω scan mode. Crystal data, data collection and refinement details for **1** and **2** are given in Table 1. The structures were solved by direct methods and refined on F^2 by full-matrix least-squares, employing Bruker's SHELXTL [24]. All non-hydrogen atoms were refined with anisotropic thermal parameters. All H atoms were placed in calculated positions, assigned fixed isotropic displacement parameters 1.2 times the equivalent isotropic U value of the attached atom, and allowed to ride on their respective parent atoms.

3. Results and discussion

3.1. Description of crystal structures

The X-ray study of [CNBzTPP][Ni(mnt)$_2$] (**1**) reveals that the molecule contains one Ni(mnt)$_2^-$ anion and one [CNBzTPP]$^+$ cation. Fig. 1 shows the molecular structure of **1**. The most relevant bond lengths and bond angles are given in Table 2. The Ni(1) of the [Ni(mnt)$_2$]$^-$ anion exhibits the square-planar coordination geometry. The Ni–S bond distances and the S–Ni–S bond angles (Table 2) within the five-membered rings agree well with those found in [Ni(mnt)$_2$]$^-$ complexes comprised of [BzTPP][Ni(mnt)$_2$] [23]. The [CNBzTPP]$^+$ cation adopts a conformation in which four phenyl rings are twisted relative to the C(14)–C(15)–P(1) reference plane, with dihedral angles of 86.3°, 89.8°, 43.9° and 124.8° for the C(9)–C(14), C(16)–C(21), C(22)–C(27) and C(28)–C(33) rings, respectively. The [Ni(mnt)$_2$]$^-$ anions in crystal form dimers *via* Ni···S and π···π stacking interactions between the Ni(mnt)$_2$ planes (Fig. 2a), and the nearest distance between S of a Ni(mnt)$_2$ plane and the Ni of the neighboring one is 3.731 Å. The mode of overlapping of [Ni(mnt)$_2$]$^-$ anions with a Ni···Ni distance of 4.725 Å is shown in Fig. 2b. As shown in Fig. 2c, there are two weak H-bonding interactions between [Ni(mnt)$_2$]$^-$ anion and adjacent [CNBzTPP]$^+$ cation. One is a weak intramolecular C(23)–H(23)···Ni(1) H-bonding interaction, with a C(23)···Ni(1) distance of 3.754 Å. Although regular weak hydrogen bonding is very common, weak hydrogen bond-

Table 3
Selected bond lengths (Å) and bond angles (°) for **2**

Bond length (Å)			
Ni(1)–S(1)	2.143(1)	S(1)–C(2)	1.714(3)
Ni(1)–S(2)	2.140(1)	S(2)–C(3)	1.721(3)
Ni(1)–S(3)	2.147(1)	S(3)–C(6)	1.712(3)
Ni(1)–S(4)	2.144(1)	S(4)–C(7)	1.715(3)
Ni(2)–S(5)	2.144(1)	S(5)–C(10)	1.713(3)
Ni(2)–S(6)	2.145(1)	S(6)–C(11)	1.711(3)
Ni(2)–S(7)	2.139(1)	S(7)–C(14)	1.721(3)
Ni(2)–S(8)	2.138(1)	S(8)–C(15)	1.719(3)
N(1)–C(1)	1.138(4)	P(1)–C(23)	1.806(2)
N(2)–C(4)	1.139(5)	P(1)–C(29)	1.785(3)
N(3)–C(5)	1.138(4)	P(1)–C(35)	1.785(3)
N(4)–C(8)	1.139(4)	P(1)–C(41)	1.787(2)
N(5)–C(9)	1.142(4)	P(2)–C(48)	1.808(3)
N(6)–C(12)	1.131(4)	P(2)–C(54)	1.782(3)
N(7)–C(13)	1.143(5)	P(2)–C(60)	1.786(3)
N(8)–C(16)	1.136(5)	P(2)–C(66)	1.795(3)
Bond angles (°)			
S(1)–Ni(1)–S(2)	92.14(3)	P(1)–C(23)–C(22)	114.7(2)
S(1)–Ni(1)–S(4)	87.39(3)	P(1)–C(29)–C(24)	120.0(3)
S(2)–Ni(1)–S(3)	88.23(4)	P(1)–C(29)–C(28)	120.3(3)
S(3)–Ni(1)–S(4)	92.27(5)	P(1)–C(35)–C(30)	122.3(2)
S(5)–Ni(2)–S(6)	92.56(3)	P(1)–C(35)–C(34)	118.6(2)
S(5)–Ni(2)–S(8)	87.59(3)	P(1)–C(41)–C(36)	121.4(2)
S(6)–Ni(2)–S(7)	87.69(3)	P(1)–C(41)–C(40)	119.8(2)
S(7)–Ni(2)–S(8)	92.17(3)	P(2)–C(48)–C(47)	115.50(18)
Ni(1)–S(1)–C(2)	103.75(9)	P(2)–C(54)–C(49)	120.11(19)
Ni(1)–S(2)–C(3)	103.43(9)	P(2)–C(54)–C(53)	120.3(2)
Ni(1)–S(3)–C(6)	103.46(9)	P(2)–C(60)–C(55)	120.85(18)
Ni(1)–S(4)–C(7)	103.59(9)	P(2)–C(60)–C(59)	119.16(18)
Ni(2)–S(5)–C(10)	103.35(9)	P(2)–C(66)–C(61)	122.4(2)
Ni(2)–S(6)–C(11)	103.24(9)	P(2)–C(66)–C(65)	118.1(2)
Ni(2)–S(7)–C(14)	103.55(11)	C(23)–P(1)–C(29)	109.99(14)
Ni(2)–S(8)–C(15)	103.55(11)	C(48)–P(2)–C(54)	110.07(14)

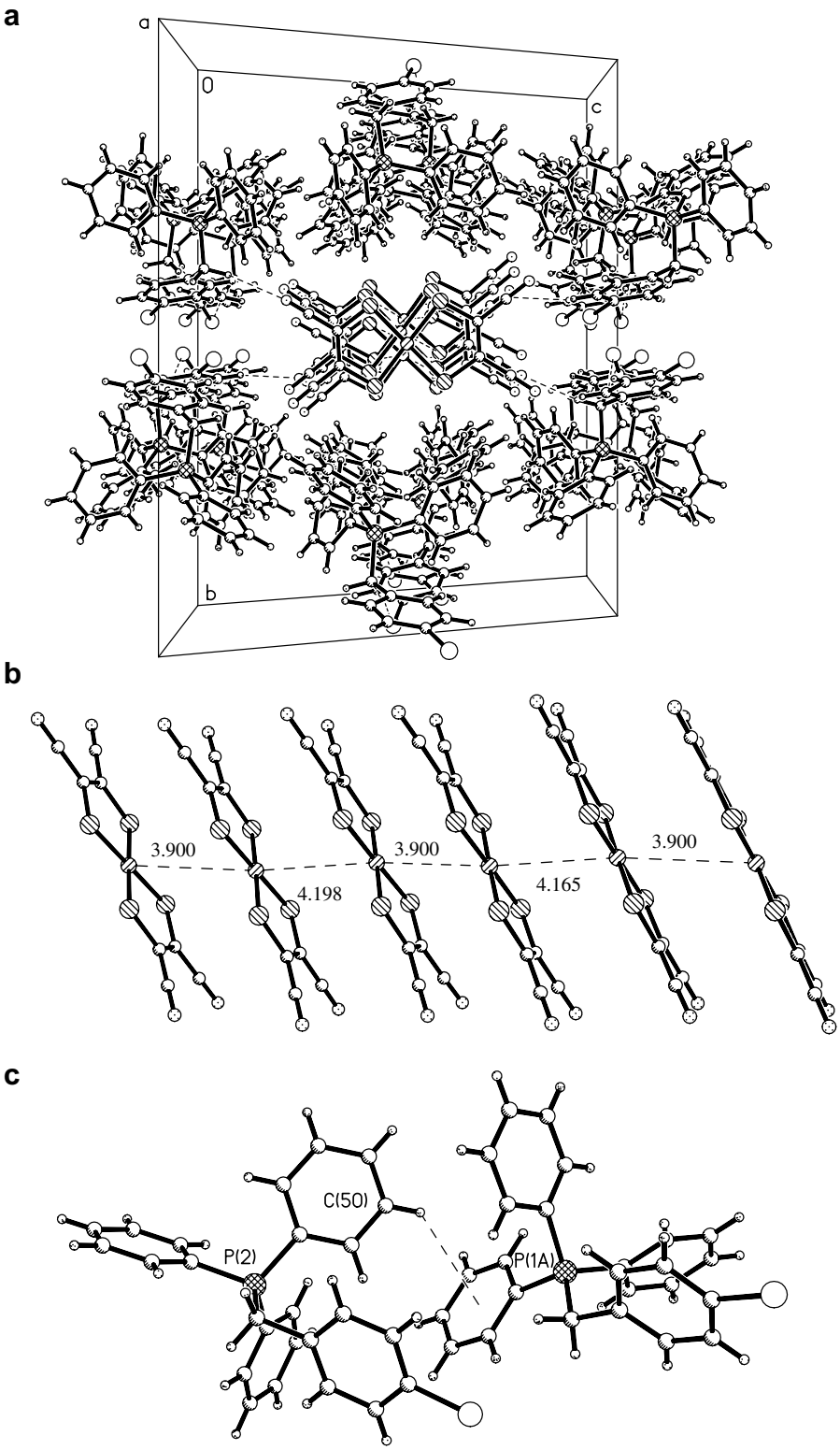

Fig. 4. (a) Packing diagram of a unit cell for **2** as viewed along *a*-axis. (b) Side view of the anions stack of **2** showing the alternating space linear-chain of $[Ni(mnt)_2]^-$ anions. (c) The C–H···π interactions between the cations for **2**.

ing with Ni is rare [25], which is similar to the C–H···Cu interactions found in the literature [26,27]. Another is an intermolecular C(10)–H(10)···N(4) interaction with a C(10)···N(4) distance of 3.255 Å.

Compound **2** crystallizes in monoclinic lattice and an asymmetric unit in a cell comprises an ion pair of $[Ni(mnt)_2]^-$ anion and $[ClBzTPPl]^+$ cation as shown in Fig. 3. The coordination geometry of anion and the confor-

Table 4
Hydrogen bonds for **1** and **2**

D–H···A	*d*(D···H) (Å)	*d*(H···A) (Å)	*d*(D···A) (Å)	∠(DHA) (°)
Compound 1				
C(10)–				
H(10)···N(4)#1	0.93	2.58	3.255(6)	130.0
Compound 2				
C(18)–				
H(18)···N(3)#2	0.93	2.58	3.366(4)	142.0
C(48)–				
H(48A)···N(6)#3	0.97	2.60	3.424(7)	143.0
C(48)–				
H(48B)···Cl(1)#4	0.93	2.59	3.447(5)	152.0

Symmetry transformations used to generate equivalent atoms: #1: $-x$, $-y+1$, $-z.+1$. #2: $x-1$, $-y+3/2$, $z-1/2$. #3: $x+1$, $-y+3/2$, $z+1/2$. #4: $-x+1$, $y-1/2$, $-z+3/2$.

mation of cation in **2** are essentially identical to those described above for **1** (the most relevant bond lengths and bond angles are listed in Table 3), while the stacking pattern of anions and cations for **2** (Fig. 4a) is significantly different from those of **1**. The Ni(III) ions form a 1D chain within a $[Ni(mnt)_2]^-$ column through intermolecular Ni···S, S···S, Ni···Ni or π···π interactions (Fig. 4b). Within a $[Ni(mnt)_2]^-$ anions stacking column, the nearest Ni···S and S···S distances are 3.615 Å and 3.807 Å, respectively, and the Ni···Ni distance alternates from 3.900 Å, 4.198 Å, 3.900 Å to 4.165 Å with the repeating periodicity of four. Because the cationic stacks mediate the anionic stacks, the closest Ni···Ni separation between anion columns is 14.374 Å, which is much longer than that of intra-stack. As a result, **2** should possess the ideal 1D alternating magnetic chain characteristic from the viewpoint of the crystal structure. As shown in Fig. 4c and Table 4, four weak H-bonding interactions such as C(18)–H(18)···N(3), C(48)–H(48A)···N(6), C(48)–H(48b)···Cl(1) and C(50)–H(50)···π are found in the solid of **2**.

By comparing the structures of **1** and **2**, we conclude that the stacking and overlapping modes are different when we have changed the *p*-substituted group in the benzene of benzyl group, and the Cl group favors separated columnar molecular stacks of anions and cations, and the CN group favors a pair of anions into dimer. In addition, some intermolecular contacts of hydrogen bonds such as C–H···N, C–H···Cl, C–H···Ni and C–H···π found between the adjacent cations and anions may play important roles in the molecular stabilizing and stacking of **1** and **2**.

3.2. Magnetic properties of *1* and *2*

The temperature dependence of the magnetic susceptibilities for **1** and **2** was measured under an applied field of 2000 Oe in the temperature range of 1.8–300 K. The plots of χ_m versus T for **1** and **2** are shown in Fig. 5 with χ_m being the magnetic susceptibility per nickel atom corrected by the diamagnetic contribution. At 300 K, the $\chi_m T$ values of **1** and **2** are 0.270, 0.201 emu K mol^{-1}, the values are lower than the expected for magnetically isolated Ni(III) ions. As the temperature is lowered, compound **1** exhibits an activated magnetic behavior in the high-temperature range together with a Curie tail at lower temperature range due to magnetic impurities, and **2** shows a magnetic behavior corresponding to a paramagnetic system with an antiferromagnetic coupling interaction.

The dinuclear model formula (1) (the Hamiltonian being $H=-2JS_AS_B$) [28] can be used to fit the magnetic susceptibilities of **1**:

$$\chi_m = (2N\beta^2g^2/kT)(1-\rho)/(3+\exp(-2J/kT)) + (N\beta^2g^2/2kT)\rho + \chi_0 \quad (1)$$

where N, g, k, β and ρ have their usual meanings [28], and J is the exchange coupling parameter describing the magnetic interaction between any two neighboring $S=1/2$ spins. The best-fit parameters obtained by least-squares fit are: $g=1.96$, $J=-441.5$ cm^{-1}, $\rho=8.3\times10^{-3}$, $\chi_0=4.0\times10^{-5}$ emu mol^{-1} and $R=1.8\times10^{-5}$ (R is defined as $\sum(\chi_m^{calcd}-\chi_m^{obsd})^2/(\chi_m^{obsd})^2$). Since the Ni···Ni distances (4.198 Å and 4.165 Å) of anions in **2** are larger than that (3.900 Å) of other anions in nickel(III) ion chains, therefore the nickel(III) ions magnetic interactions can be neglected,

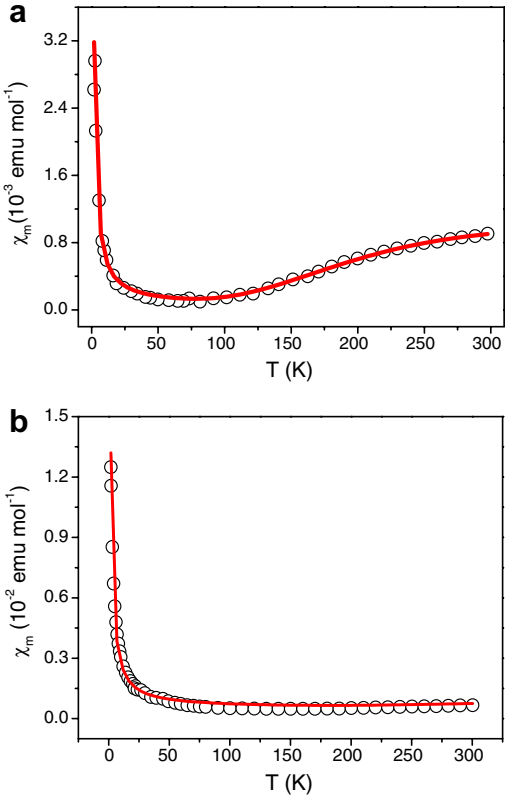

Fig. 5. Plots of χ_m vs. T for **1** (a) and **2** (b). The red solid line is reproduced from the theoretical calculations, and detailed fitting procedure is described in the text. (For interpretation of the references to color in this figure legend, the reader is referred to the web version of this article.)

and the magnetic susceptibility data of **2** can also be analyzed using simple dinuclear model (Eq. (1)). The best-fit parameters are: $g = 1.98$, $J = -830.0\ \mathrm{cm}^{-1}$, $\rho = 3.1 \times 10^{-2}$, $\chi_0 = 5.1 \times 10^{-4}$ emu mol^{-1} and $R = 6.1 \times 10^{-6}$. The model provides an excellent fit for **1** and **2** (the solid lines in Fig. 5a and b), as indicated by the low value of R.

4. Conclusions

In conclusion, the crystal structures and magnetic properties were presented for two novel molecular magnetic materials containing the $Ni(mnt)_2^-$ anion. The $Ni(mnt)_2^-$ anions of **1** form dimer *via* Ni···S and π···π stacking interactions between $Ni(mnt)_2$ planes, but the anions and cations of **2** stack into well-segregated columns in the solid state; and the Ni(III) ions form a 1D alternating chain in a $Ni(mnt)_2$ column through intermolecular Ni···S, or π···π interactions. Magnetic susceptibility measurements for these complexes show that the overall magnetic behavior for **1** and **2** indicates the presence of antiferromagnetic interaction, but **1** exhibits an activated magnetic behavior in the high-temperature (HT) region together with a Curie tail in the low-temperature (LT) region.

5. Supplementary material

CCDC 636259 and 636260 contain the supplementary crystallographic data for **1** and **2**. These data can be obtained free of charge via http://www.ccdc.cam.ac.uk/conts/retrieving.html, or from the Cambridge Crystallographic Data Centre, 12 Union Road, Cambridge CB2 1EZ, UK; fax: (+44) 1223-336-033; or e-mail: deposit@ccdc.cam.ac.uk.

Acknowledgement

The authors are grateful for the president's foundation of South China Agricultural University (No. 2005K092).

References

[1] A.T. Coomber, D. Beljonne, R.H. Friend, J.L. Brédas, A. Charlton, N. Robertson, A.E. Underhill, M. Kurmoo, P. Day, Nature 380 (1996) 144.
[2] T. Akutagawa, T. Nakamura, Coord. Chem. Rev. 226 (2002) 3.
[3] N. Robertson, L. Cronin, Coord. Chem. Rev. 227 (2002) 93.
[4] T. Akutagawa, T. Motokizawa, K. Matsuura, S. Nishihara, S.I. Noro, T. Nakamura, J. Phys. Chem. 12 (2006) 5897.
[5] N. Hideyasu, K. Mao, A. Minoru, K. Tadashi, M. Takehiko, Inorg. Chem. 43 (2004) 6075.
[6] M. Urichi, K. Yakushi, Y. Yamashita, J. Qin, J. Mater. Chem. 8 (1998) 141.
[7] P.I. Clemenson, A.E. Underhill, M.B. Hursthouse, R.L. Short, J. Chem. Soc., Dalton Trans. (1988) 1689.
[8] J. Nishijo, E. Ogura, J. Yamaura, A. Miyazaki, T. Enoki, T. Takano, Y. Kuwatani, M. Iyoda, Solid State Commun. 116 (2000) 661.
[9] J.L. Xie, X.M. Ren, Y. Song, W.W. Zhang, W.L. Liu, C. He, Q.J. Meng, Chem. Commun. (2002) 2346.
[10] J.L. Xie, X.M. Ren, Y. Song, Y. Zou, Q.J. Meng, J. Chem. Soc., Dalton Trans. (2002) 2868.
[11] X.M. Ren, Q.J. Meng, Y. Song, C.S. Lu, C.J. Hu, Inorg. Chem. 41 (2002) 5686.
[12] J.L. Xie, X.M. Ren, S. Gao, W.W. Zhang, Y.Z. Li, C.S. Lu, C.L. Ni, W.L. Liu, Q.J. Meng, Y.G. Yao, Eur. J. Inorg. Chem. (2003) 2393.
[13] C.L. Ni, D.B. Dang, Y. Song, S. Gao, Y.Z. Li, Z. P Ni, Z.F. Tian, L.L. Wen, Q.J. Meng, Chem. Phys. Lett. 396 (2004) 353.
[14] Z.P. Ni, X.M. Ren, J. Ma, J.L. Xie, C.L. Ni, Z.D. Chen, Q.J. Meng, J. Am. Chem. Soc. 127 (2005) 14330.
[15] C.L. Ni, D.B. Dang, Y.Z. Li, S. Gao, Z.P. Ni, Z.F. Tian, Q.J. Meng, J. Solid State Chem. 178 (2005) 100.
[16] C.L. Ni, Y.Z. Li, D.B. Dang, Y. Song, Z.P. Ni, Q.J. Meng, Inorg. Chim. Acta 358 (2005) 2680.
[17] C.L. Ni, Y. Song, Q.J. Meng, Chem. Phys. Lett. 419 (2006) 351.
[18] C.L. Ni, Z.F. Tian, Z.P. Ni, D.B. Dang, Y.Z. Li, Y. Song, Q.J. Meng, Inorg. Chim. Acta 359 (2006) 3927.
[19] C.L. Ni, D.B. Dang, Y.Z. Li, Y. Song, Z.P. Ni, Z.F. Tian, Z.R. Yuan, S. Gao, Q.J. Meng, Solid State Sci. 8 (2006) 520.
[20] C.L. Ni, X.P. Liu, L.L. Yu, L.M. Yang, J. Phys. Chem. Solid 68 (2007) 59.
[21] A. Davison, R.H. Holm, Inorg. Synth. 10 (1967) 8.
[22] S.B. Bulgarevich, D.V. Bren, D.Y. Movshovic, P. Finocchiaro, S. Failla, J. Mol. Struct. 317 (1994) 147.
[23] C.L. Ni, Y.Z. Li, Q.J. Meng, J. Coord. Chem. 58 (2005) 759.
[24] SHELXTL, Version 5.10. Structure Determination Software Programs, Bruker Analytical X-ray Systems Inc., Madison, WI, USA, 2000.
[25] S.B. Yang, C.L. Ni, Acta Crystallogr., Sect. E 60 (2006) 483m.
[26] D. Braga, F. Grepioni, E. Tegesco, K. Biradha, G.R. Desiraju, Organometallics 16 (1997) 846.
[27] L.Y. Yang, Q.Q. Chen, Y. Li, S.X. Xiong, G.P. Li, J.S. Ma, Eur. J. Inorg. Chem. (2004) 1478.
[28] Y. Song, D.R. Zhu, K.L. Zhang, Y. Xu, C.Y. Duan, X.Z. You, Polyhedron 19 (2000) 1461.